Supporting Information for

A Series of Polyoxometalates–Based COF Composites by One–Pot Mechanosynthesis for Thioether to Sulfone

Yanyan Guo, Xiaohui Liu, Xiaodong Liu, Na Xu,* Xiuli Wang*

College of Chemistry and Materials Engineering, Bohai University, Liaoning Professional Technology Innovation Center of Liaoning Province for Conversion Materials of Solar Cell, Jinzhou 121013, P. R. China

Table of Contents

Experimental section

Materials and methods

1, 3, 5–triformylphloroglucinol (Tp), p–phenylenediamine (Pa–1) were purchased from Jilin Research and Extension Technology Company. Keggin–type $H_3PMo_{12}O_{40}$ (PMo_{12}), $H_3PW_{12}O_{40}$ (PW_{12}), $H_3SiW_{12}O_{40}$ (SiW_{12}), mesitylene, 1,4–dioxane were all purchased by Aladdin Reagents. Powder X–ray diffraction (PXRD) patterns of the samples were measured by a D/teX Ultra diffractometer with Cu Kα radiation (λ = 1.5418 Å). FT–IR spectra were carried out on a Perkin Elmer Spectrum. Thermogravimetric analyses were conducted using a Hitachi TG/DTA7200 analyzer in an N_2–flow atmosphere with a heating rate of 10 ℃/min at a temperature of 25–800 ℃. Scanning electron microscope images (SEM) and energy–dispersive spectroscopy (EDS) were conducted on a cold field–emission scanning electron microscope (S–4800). Transmission electron microscope (TEM) (JEOL JEM–2100F, 200 kV) equipped with EDS (X–MaxN 80T IE250). The planetary ball mill (QM–3SP04) is from Nanjing Nanda Instrument Company. The catalytic reaction was analyzed by using a Shimadzu Tech–comp GC–7900 gas chromatograph (GC) with a flame ionization detector equipped with a TM–5 Sil capillary column.

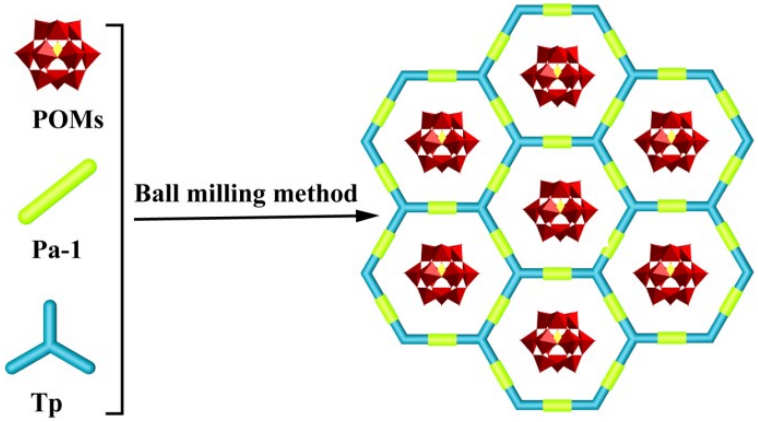

Fig. S1 Schematic illustration for the syntheses of POMs@TpPa–1.

Fig. S2 (a) The pictures of TpPa–1; (b) PW_{12}@TpPa–1; (c) PMo_{12}@TpPa–1.

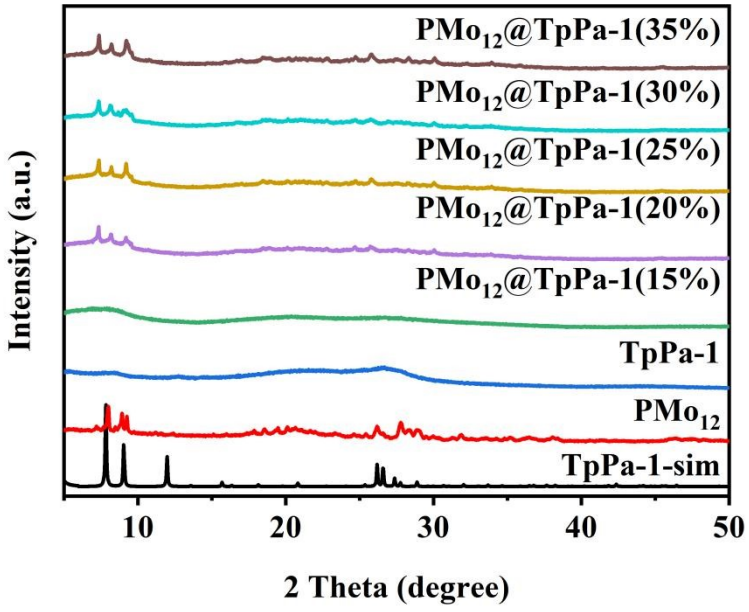

Fig. S3 PXRD patterns of PMo_{12}, TpPa–1 and PMo_{12}@TpPa–1.

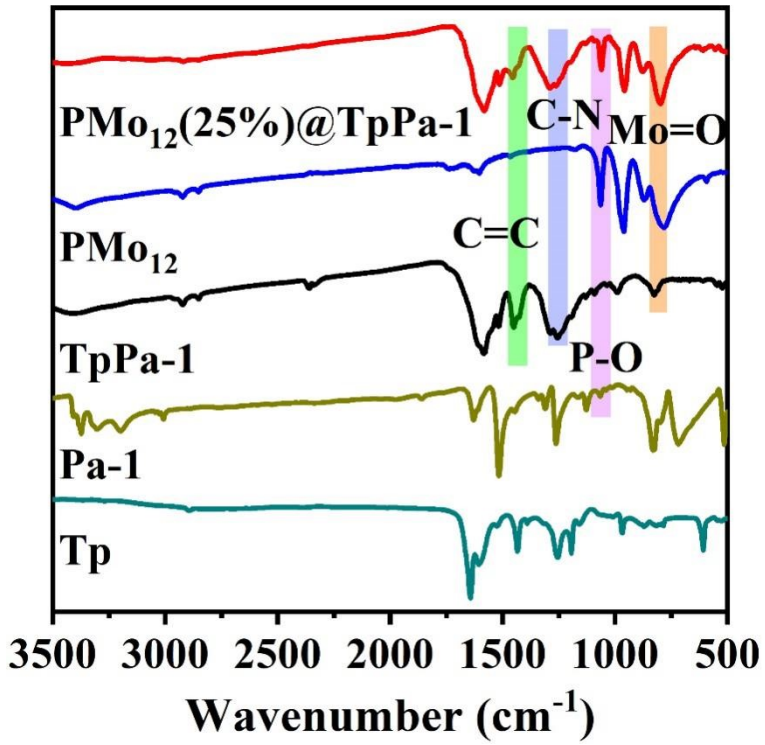

Fig. S4 IR spectra of monomer, TpPa–1, PMo_{12}@TpPa–1 and PMo_{12}.

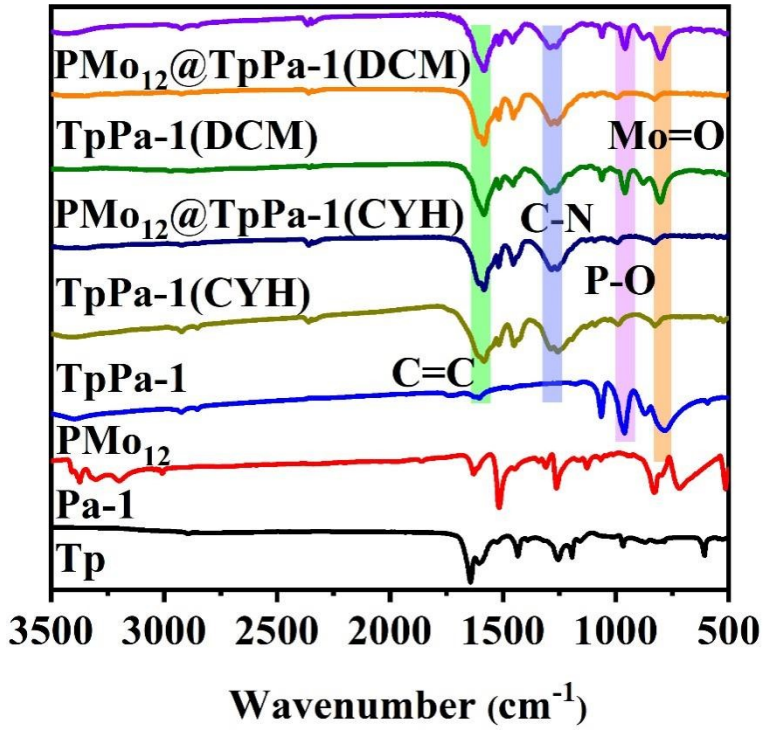

Fig. S5 IR spectra of monomer, TpPa–1, PMo_{12}@TpPa–1 and PMo_{12} in CYH and DCM.

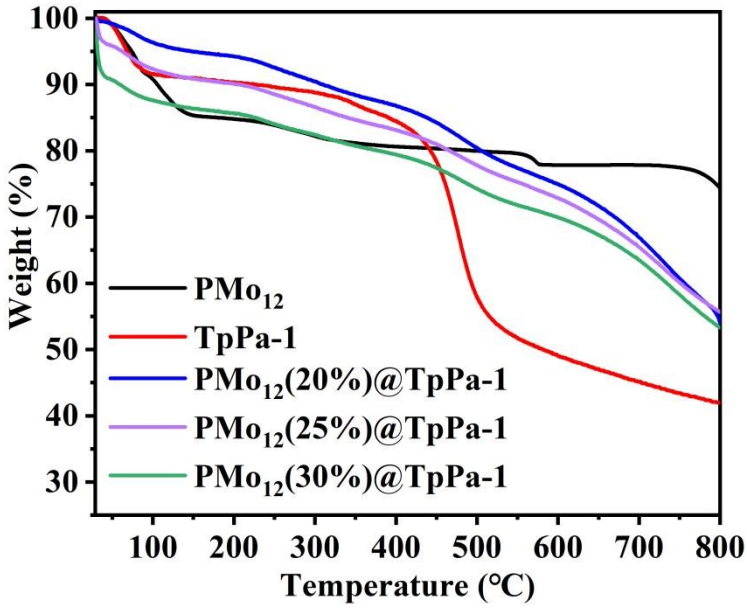

Fig. S6 TGA of TpPa–1, PMo_{12}@TpPa–1 and PMo_{12}.

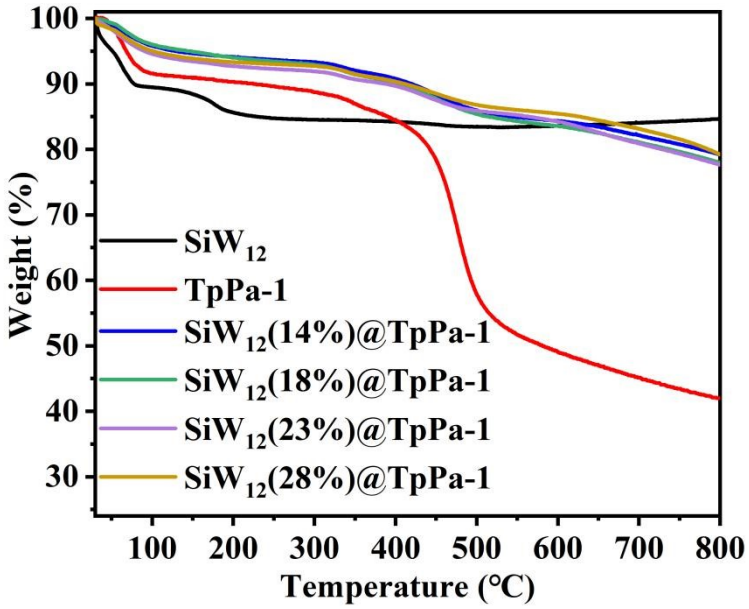

Fig. S7 TGA of TpPa–1, SiW_{12}@TpPa–1 and PMo_{12}.

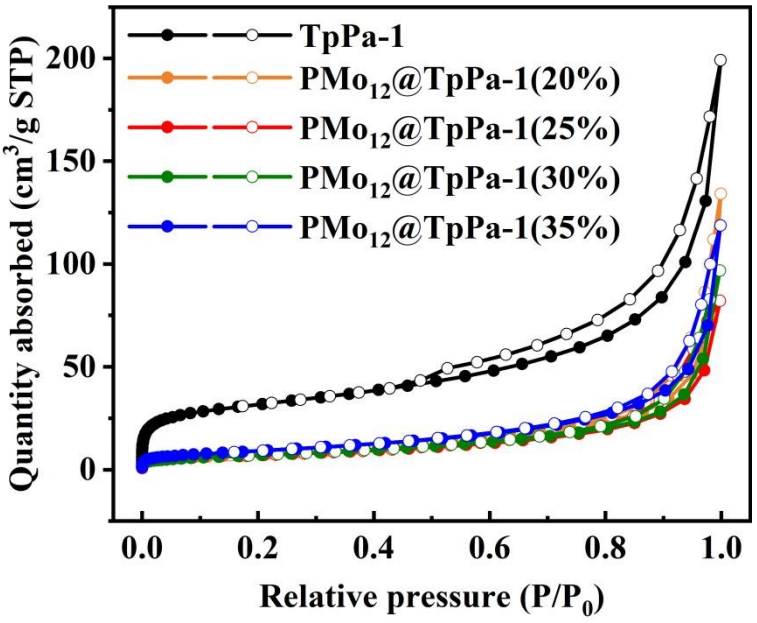

Fig. S8 N_2 sorption isotherms of TpPa–1 and different PMo_{12} added amounts of PMo_{12}@TpPa–1 measured at 77 K.

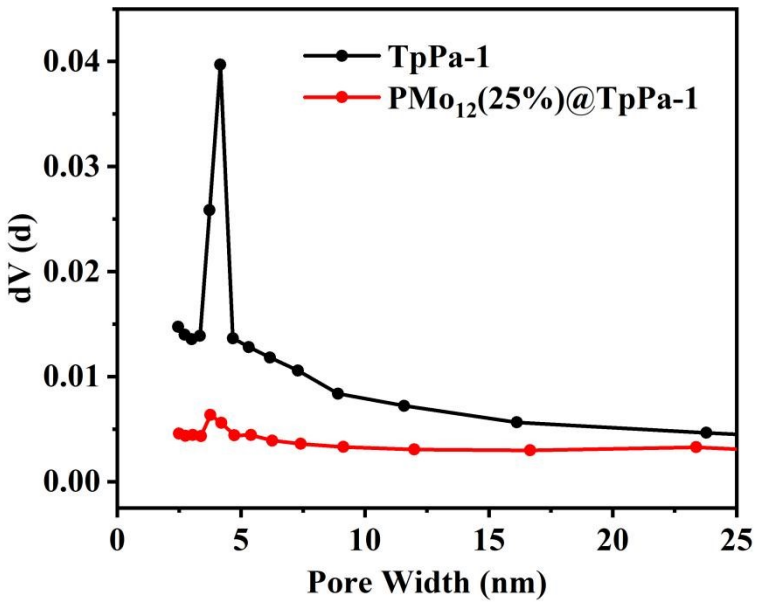

Fig. S9 The pore size distribution of TpPa–1 and PMo_{12}(25%)@TpPa–1.

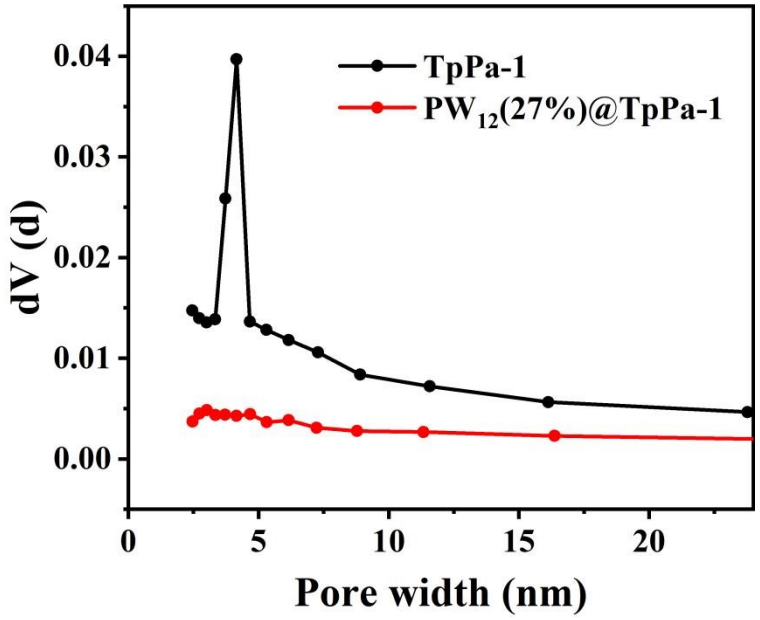

Fig. S10 The pore size distribution of TpPa–1 and PW_{12}(27%)@TpPa–1.

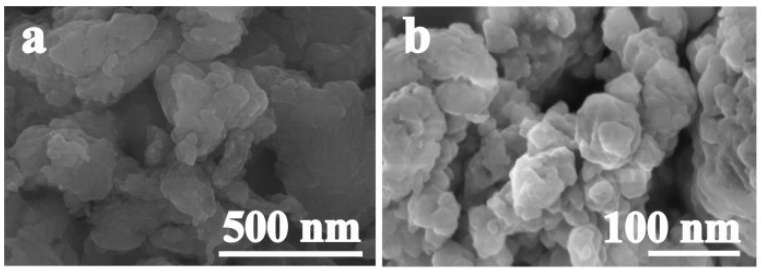

Fig. S11 (a) SEM characterization of TpPa–1; (b) SEM characterization of PW_{12}@TpPa–1.

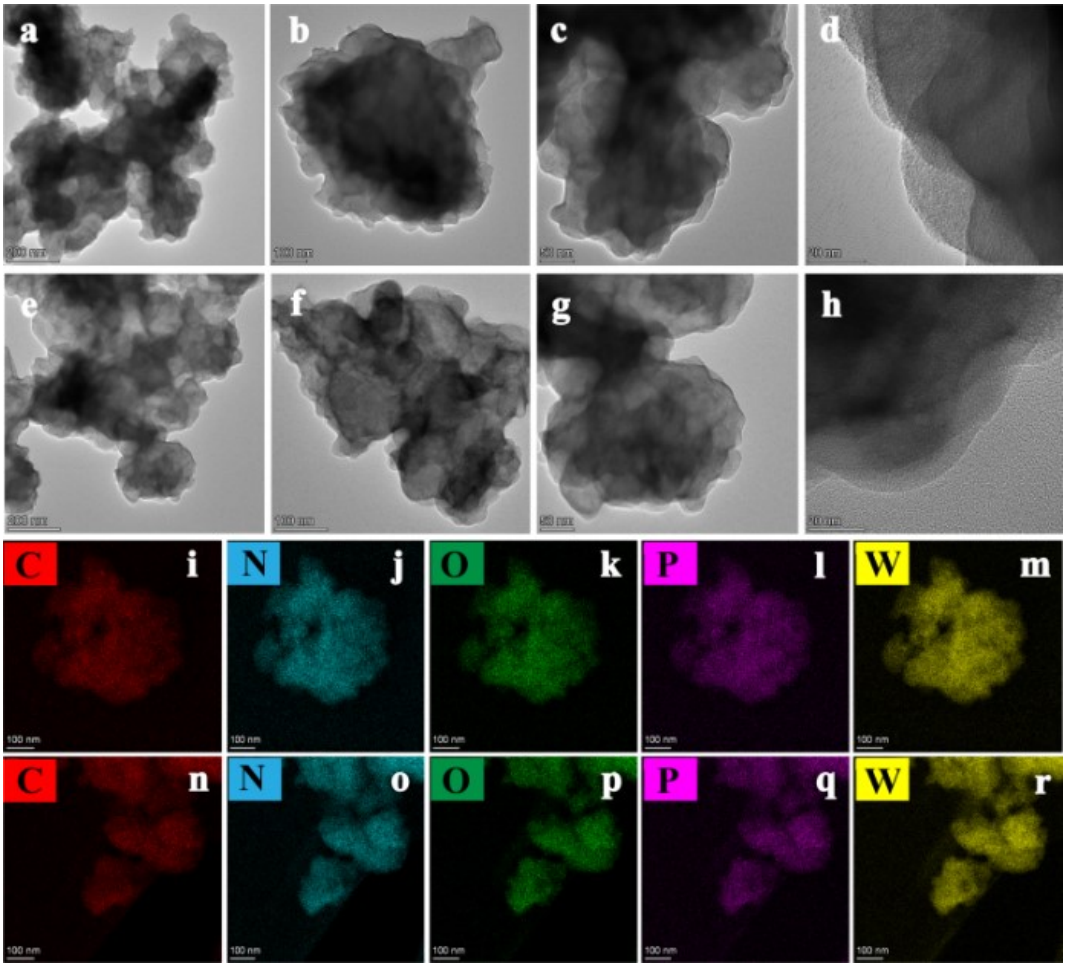

Fig. S12 (a–d) TEM characterization of PW_{12}(22%)TpPa–1; (e–h) TEM characterization of PW_{12}(32%)TpPa–1; (i–m) EDS characterization of PW_{12}(22%)@TpPa–1; (n–r) EDS characterization of PW_{12}(32%)@TpPa–1.

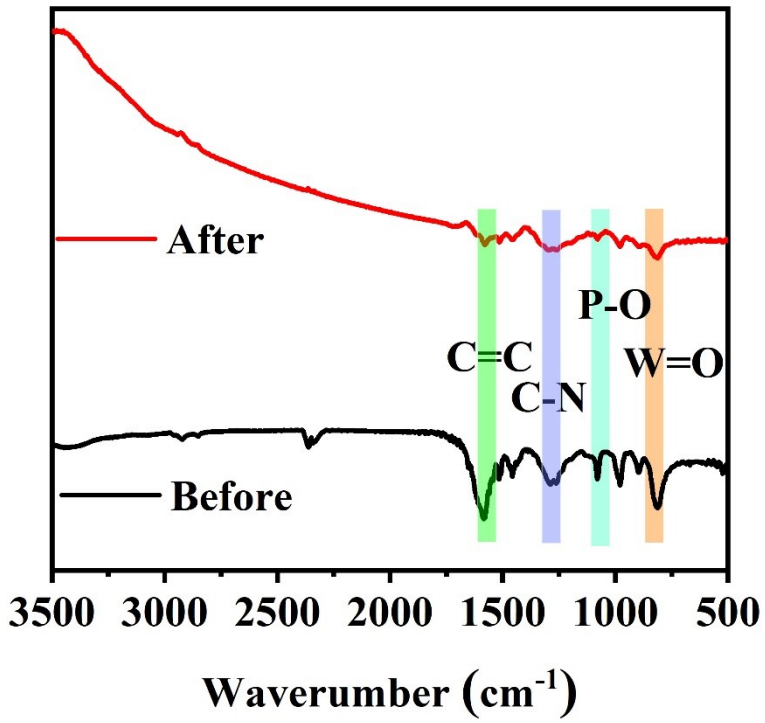

Fig. S13 FT–IR spectra of PW_{12}(27%)@TpPa–1 before and after three runs catalytic reactions in the characteristic regions.

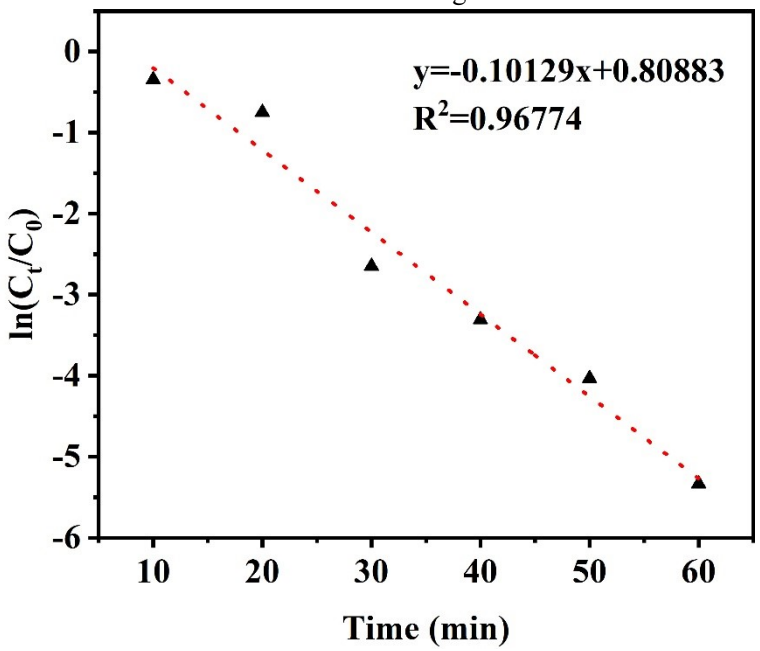

Fig. S14 Reaction rate plots for MPS using PW_{12}(27%)@TpPa–1 as the catalyst.

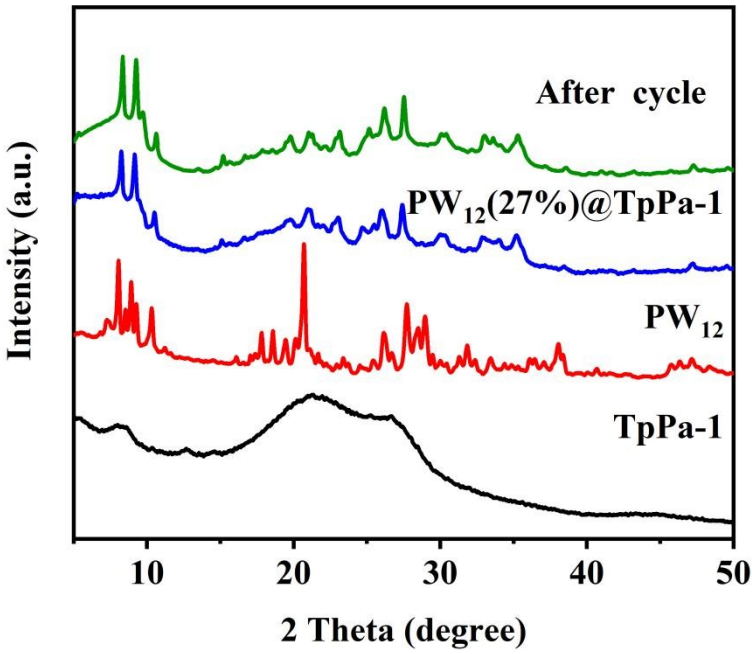

Fig. S15 PXRD spectra of PW_{12}(27%)@TpPa–1 before and after cycle catalytic reactions.

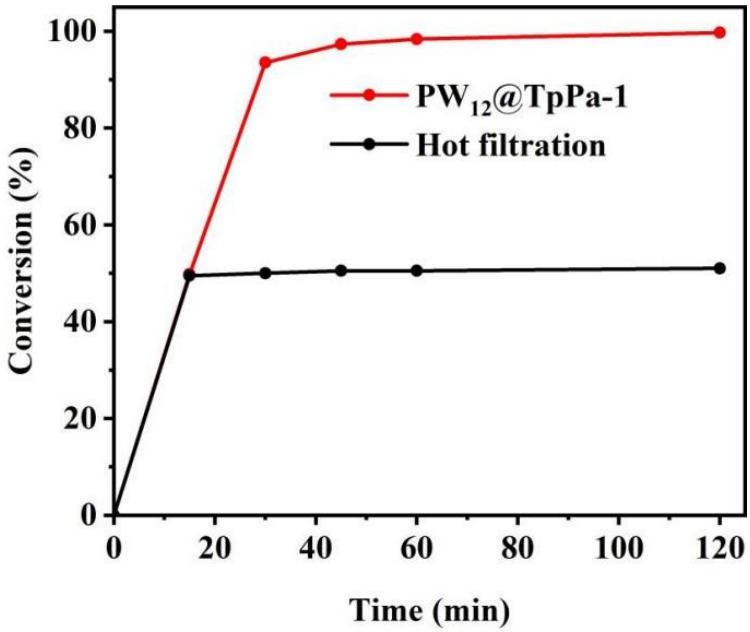

Fig. S16 Hot filtration of PW_{12}(27%)@TpPa–1 in the oxidation of MPS.

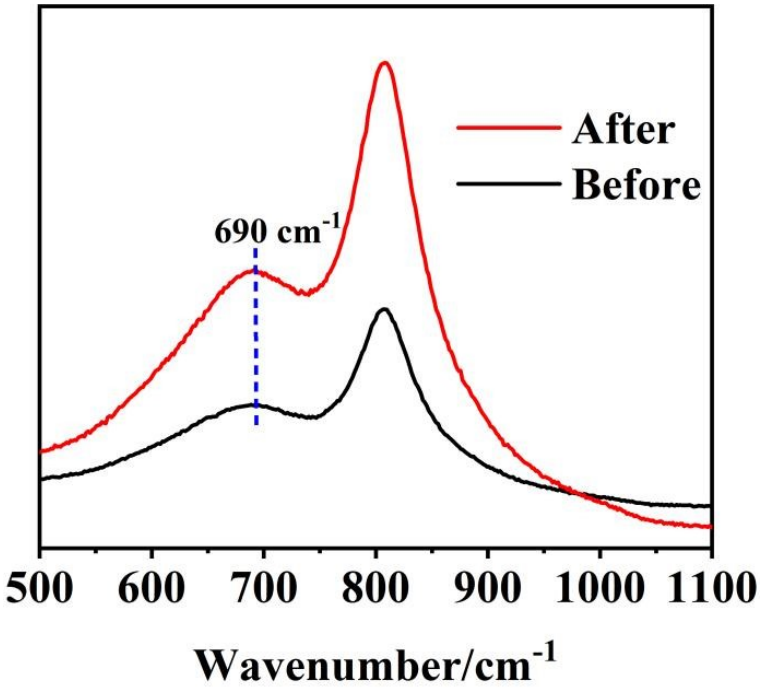

Fig. S17 Raman spectra of PW_{12}(27%)@TpPa–1 before and after treating with H_2O_2.

Table S1 Physicochemical properties of PW_{12}@TpPa–1 composites.

Composites	S_{BET} (m^2/g)	Vtotal (cc/g)	Average pore size (nm)
TpPa–1	91.81	0.28	6.16
PW_{12}(22%)@TpPa–1	11.41	0.11	19.95
PW_{12}(27%)@TpPa–1	21.52	0.10	8.84
PW_{12}(32%)@TpPa–1	9.60	0.08	17.42
PMo_{12}(20%)@TpPa–1	28.39	0.21	14.61
PMo_{12}(25%)@TpPa–1	25.22	0.13	10.1
PMo_{12}(30%)@TpPa–1	26.05	0.15	11.5

Table S2 Comparison with other reported catalysts for MPS oxidation.

Cat.	Temp. (℃)	Time (min)	Conv. (%)	Sel. (%)	Ref
PW_{12}@TpPa-1	**60**	**60**	**99.5**	**100**	**This work**
$(Hbiz)_{12}[(P_2Co_2Mo^{V}_4O_8)_2(P_2Mo^{V}_2O_8)_4(Pb\subset P_6Co_2Mo^{V}_2Mo^{VI}_{14}O_{73})_4]\cdot ca.129H_2O$	60	80	99.1	98.7	1
VO–TAPT–2,3–DHTA COFs	25	240	93.0	90.0	2
$KTaxTi1–xO_3$	60	240	87.0	80.0	3
Ag–DTMH	50	120	99.0	94.0	4
Ni–DTMH	40	180	96.0	63.0	4
Co–DTMH	40	180	31.0	99.0	4
V/MCM–41	25	360	80.0	93.0	5

Table S3 The oxidation of MPS using different catalystsa.

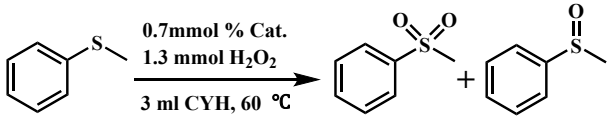

Entry	Catalyst	System	Conv. (%)	Sel.[b] (%)
1	PW_{12}(22%)@TpPa–1	Heterogeneous	92.3	87.0
2	PW_{12}(32%)@TpPa–1	Heterogeneous	95.2	97.8
3	PW_{12}(37%)@TpPa–1	Heterogeneous	89.4	97.0
4	[d]PW_{12}(27%)@TpPa–1	Heterogeneous	92.0	99.1
5	[e]PW_{12}(27%)@TpPa–1	Heterogeneous	93.5	94.8
6	[f]PW_{12}(27%)@TpPa–1	Heterogeneous	**99.5**	**100**
7	[g]PW_{12}(27%)@TpPa–1	Heterogeneous	92.4	98.3
8	[h]PW_{12}(27%)@TpPa–1	Heterogeneous	83.1	89.0
9	PMo_{12}(20%)@TpPa–1	Heterogeneous	74.5	77.0
10	PMo_{12}(30%)@TpPa–1	Heterogeneous	86.6	86.5
11	SiW_{12}(14%)@TpPa–1	Heterogeneous	76.0	44.4
12	SiW_{12}(18%)@TpPa–1	Heterogeneous	89.4	81.5
13	SiW_{12}(23%)@TpPa–1	Heterogeneous	85.5	68.4
14	SiW_{12}(28%)@TpPa–1	Heterogeneous	69.0	60.0

[a]Reaction conditions: 0.5 mmol MPS; 0.7 mmol% catalyst; 3 mL CYH; 1.3 mmol H_2O_2; 60 ℃; 60 min. [b]Selectivity to sulfone, the byproduct was sulphones. [c]Selectivity to sulfoxides, the byproduct was sulphones. [d-h]The amount of catalyst added was 0.5 mmol%, 0.6 mmol%, 0.7 mmol%, 0.8 mmol%, and 0.9 mmol% respectively.

Table S4 Selective oxidation of various sulfides to sulfoxide[a].

Entry	Substrate	Temp. (℃)	Time (min)	Conv. (%)	Sel.[b] (%)
1	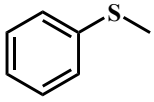	60	60	99.0	99.0
2	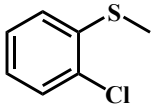	60	60	97.0	98.0
3	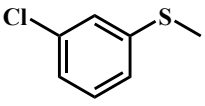	60	60	85.2	92.7
4	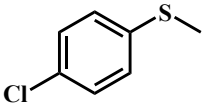	60	60	97.8	98.2

5	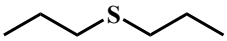	60	60	84.06	99.0
6	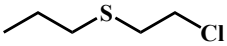	60	60	88.8	59.3

[a]Reaction conditions: 0.5 mmol sulfide; 0.7 mmol% catalyst; 3 mL CYH; 1.3 mmol H_2O_2; 60 ℃; 60 min. [b]Selectivity to sulfone, the byproduct was sulfoxides.

references

1. X. Liu, N. Xu, X. Liu, Y. Guo, X. Wang, *Chem Commun (Camb).*, 2022, **58**, 12236-12239.
2. H. Vardhan, G. Verma, S. Ramani, A. Nafady, A. M. Al–Enizi, Y. Pan, Z. Yang, H. Yang, S. Ma, *ACS Appl Mater Inter.,* 2019, **11**, 3070–3079.
3. C. Leal Marchena, G. Pecchi, L. Pierella, *Molecular Catalysis.,* 2020, **482**.
4. X. Huang, X. Gu, Y. Qi, Y. Zhang, G. Shen, B. Yang, W. Duan, S. Gong, Z. Xue, Y. Chen, *Chin. J. Chem.,* 2021, **39**, 2495-2503.
5. T. Ben Zida, I. Khedhera, J.M. Fraileb. *Journal of Chemical Research.,* 2013, **37(12)**, 766-773.